

*Regular article***Numerical flow-field analysis and design optimization of a high-energy first-stage centrifugal pump impeller**

F.C. Visser, R.J.H. Dijkers, J.G.H. op de Woerd

Flowsolve, Rotating Equipment Division, P.O. Box 25, NL – 4870 AA Etten-Leur, The Netherlands

Received: 1 March 1999/Accepted: 21 September 1999

Communicated by: M. Espedal and A. Quarteroni

**Abstract.** Described is the numerical flow-field analysis and design optimization of the first-stage impellers of a so-called high-energy centrifugal pump having two single-suction first-stage impellers and one double-suction second stage impeller. This study has been carried out with the aid of three-dimensional computational-fluid-dynamics calculations, employing the potential-flow approximation of the governing equations. The study was conducted because the first-stage impellers of the pump considered appeared to suffer from severe premature wear due to cavitation attack on the vane leading edges, which situation had to be improved. The analysis carried out for the existing design produced suggestions for improvement, and based on these suggestions a new first-stage impeller design was developed. Subsequently, this new design was numerically analyzed to substantiate its potentially better (cavitation) performance. It appeared that the blade inlet angle of the original impeller design was too excessive at mid span, causing best cavitation performance to occur at 160 percent of the rated flow. The new design has its best cavitation point at the rated flow, and will not suffer from premature wear due to cavitation attack like the existing design.

**1 Introduction**

Cavitation is one of the most important aspects that needs to be considered in designing centrifugal pumps, since it is a major contributor to failure and/or inefficiency in these rotating fluid-handling machines (see for instance [2]). As cavitation occurs, performance is lost and/or pump (impeller) life is reduced.

Due to this physical phenomenon, pumps sizes ( $L$ ) and rotational speeds ( $\Omega$ ) are limited, since velocities ( $\Omega L$ ) are limited (by the occurrence of cavitation). This directly poses a problem when pump sizes are decreased, in that rotational speed has to increase in order to get the same (desired) performance ( $\Omega L^3$ ).

Therefore, a good economic pump has optimal size and speed combined and should be running very close to the

physical limit imposed by cavitation. The currently available numerical tools and methods for impeller flow-field analysis make it possible to design closely to this limit. An example of redesigning an existing pump impeller in this way is presented in this paper.

Outlined is the numerical flow-field analysis and design optimization of the first-stage impellers of a so-called high-energy centrifugal pump. Figure 1 shows the pump considered. It comprises two single-suction first-stage impellers and one double suction second-stage impeller. The first-stage impellers of this pump appeared to suffer from premature wear due to cavitation attack on the vane leading edges. The severity of this cavitation attack is illustrated in Fig. 2. It shows the cavitation damage after just one year of operation.

In order to improve the existing situation, a detailed (three-dimensional) numerical flow-field analysis was carried out, employing the potential-flow approximation of the governing equations. Apart from the regular pressure distribution and velocity flow field, this predicted in particular cavitation inception in terms of Net Positive Suction Head (NPSH), which enabled optimization of the existing design.

The analysis carried out for the existing design, produced suggestions for improvement, and based on these suggestions a new first-stage impeller design was developed, which was subsequently numerically analyzed to substantiate its potentially better performance. From the analysis it became evident

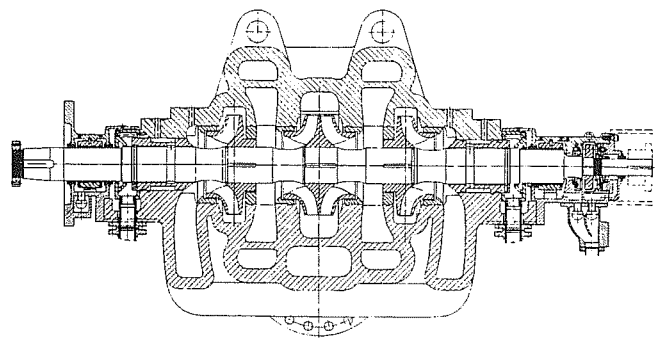


Fig. 1. Cross-sectional view of two-stage dual-first-stage centrifugal pump

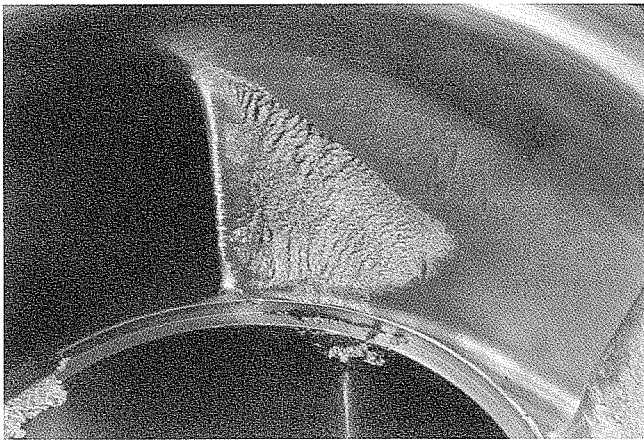


Fig. 2. Damage patterns on first-stage impeller after one year of operation

that the inlet angle of the existing impeller design was too excessive at mid span, causing best cavitation performance to occur at 160 percent of the rated flow. The new design has its best cavitation point at the rated flow, and will not suffer from premature wear due to cavitation attack like the existing design.

The plan of discussion is first to present the numerical method of cavitation inception analysis employed, including some background on *NPSH* and cavitation. Next, (operating) details of the existing pump and analysis results for the existing design will be outlined. Then, lastly, the new design and its numerically predicted performance will be discussed.

## 2 Numerical method of cavitation inception analysis

### 2.1 Background – *NPSH* and cavitation

Cavitation is defined as the process of formation and disappearance of the vapor phase of a liquid when it is subjected to reduced and subsequently increased pressures at constant ambient temperatures. The formation of cavities is a process analogous to boiling in a liquid, although it is the result of pressure reduction rather than heat addition. Nonetheless, the basic physical and thermodynamic processes are the same in both cases.

Clearly, from an engineering and design point of view there are two basic questions regarding cavitation. Firstly, one has to answer the question whether cavitation will occur or not, and secondly, if cavitation is unavoidable, the question is whether a given design can still function properly. Economic or other operational considerations often necessitate operation with some cavitation, and under these circumstances it is particularly important to understand the (deleterious) effects of cavitation.

**2.1.1 Occurrence of cavitation.** A liquid is said to cavitate when (a) vapor bubbles form and grow as a consequence of pressure reduction, and (b) vapor bubbles subsequently disappear or collapse due to a pressure increase. Such bubble formation is nearly always accompanied by production of gases previously dissolved in the liquid. The phase transition resulting from the hydrodynamic pressure changes yields a two-phase flow composed of a liquid and its vapor phase,

which is called a cavitating flow. Obviously, a cavitating flow can imply anything from the initial formation of bubbles to large-scale attached cavities (known as supercavitation). Nowadays, such cavitating flows are rather common occurrences, since designers are pushing for higher speeds for given sizes in the development of pumps (thus creating lower pressures in the suction area of the impellers).

**2.1.2 Cavitation inception and three-percent head drop.** The first appearance of cavitation is called cavitation inception. When the pressure is decreased from this inception level, the region of cavitation enlarges, eventually starting to cause noise, performance change, and possibly cavitation damage. The latter results from the fact that well beyond inception, the pressures associated with cavity collapse are high enough to cause failure of the impeller material. By the time the inlet pressure is lowered enough to cause a one to three percent drop in pump head, cavitation is usually fully established.

Above-mentioned stages of cavitation are illustrated in Fig. 3, in which the total pump head (*H*) is plotted against the net positive suction head (*NPSH*) for constant volume flow rate (*Q*) and constant angular speed (*N*). This abstraction, termed *NPSH*, is defined as the total head ( $p_0$ ) of the fluid at the suction nozzle above the vapor pressure ( $p_v$ ) of the fluid, and can be regarded as a measure for the margin against vaporization of the fluid entering the pump; i.e.

$$NPSH = \frac{p_0 - p_v}{\rho g} \quad (1)$$

where  $\rho$  is density of the fluid and  $g$  is acceleration due to gravity.

From a set of test curves like Fig. 3 it is possible to develop the *NPSH* required characteristic (say *NPSH* at three-percent head drop) as a function of the throughflow. Such is done by determining the cavitation points for three-percent head drop at different ( $Q/N$ ) operating points, i.e. at different specific flow rates  $\Phi = Q/(\Omega R^3)$ .

**2.1.3 Cavitation damage.** Cavitation damage starts somewhere between inception and three-percent head drop (Fig. 3). A more accurate description is difficult to give since many parameters influence bubble geometry and its potential for causing damage. For instance, impeller material, air content, *NPSH* available, vane geometry, inlet geometry, type of cavity, fluid density, and water temperature, to name a few, can

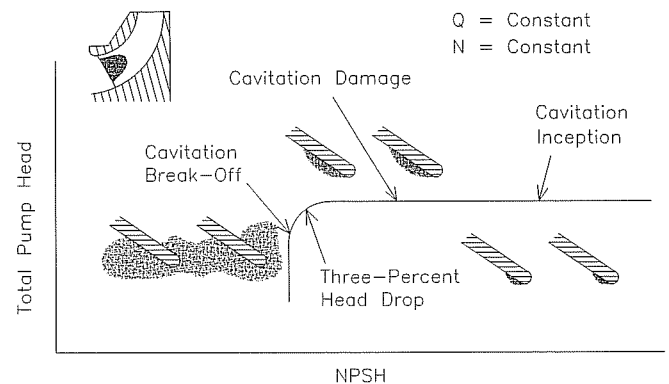


Fig. 3. Cavitation phenomena

be contributors or inhibitors of cavitation damage. The only certainty is that the absence of visible cavities means that cavitation damage will not be an issue.

## 2.2 Numerical method [6, 7]

**2.2.1 Potential-flow approximation.** The numerical method employed in this study to compute the impeller flow field, and subsequently calculate the incipient *NPSH*, is based on the potential-flow approximation of the governing equations. This means (mathematically) that the core flow is considered irrotational (i.e.  $\nabla \times \underline{v} = 0$ ) and solenoidal (i.e.  $\nabla \cdot \underline{v} = 0$ ), where  $\underline{v}$  is the fluid velocity (see for instance [4] or [1]). This assumption is justified as long as (a) the importance of the viscous forces compared to the non-viscous (inertia) forces acting upon the fluid will be small, and (b) the fluid may be regarded incompressible. An additional assumption thereby being that the fluid enters (the machine) free from vorticity. For pumping machinery these assumptions usually hold.

The (core) flow field can then be described by a velocity potential  $\phi$  obeying the relation

$$\underline{v} = \nabla \phi \quad (2)$$

while the equation of continuity reduces to the Laplace equation, i.e.

$$\nabla^2 \phi = 0 \quad (3)$$

The pressure distribution is next computed from the (unsteady) Bernoulli equation,

$$\frac{\partial \phi}{\partial t} + \frac{1}{2} \underline{v} \cdot \underline{v} + \frac{p}{\rho} + gz = c(t) \quad (4)$$

where  $t$  is time,  $p$  is thermodynamic pressure,  $z$  is elevation,  $c(t)$  and is a time-dependent constant.

The Laplace equation (3) is solved numerically by a three-dimensional finite-element method, which has been developed at the University of Twente, The Netherlands [3, 5]. Computing time and memory requirements for this method have been reduced by employing a super-element approach. In this way the internal degrees of freedom are expressed in terms of degrees of freedom that are located at the boundary of the super elements.

The speed of the potential code (solver) makes it a very convenient tool, not only for analyses (like performance and *NPSH* prediction) but also for (parametric) impeller design.

**2.2.2 Determination of incipient cavitation.** Employment of the potential-flow approximating, enables the cavitation inception point to be determined as follows.

Firstly, the flow field (i.e. the velocity and pressure distribution) is calculated for a reference pressure at the impeller inlet (say  $p_{0,\text{ref}} = 0$ ). Next, the minimum pressure  $p_{\text{min}}$  along the vanes is determined. Then, the inception inlet pressure  $p_{0,i}$  is equated by

$$p_{0,i} = p_{0,\text{ref}} - p_{\text{min}} + p_v \quad (5)$$

Substituting this in (1) gives that the incipient *NPSH* can readily be computed by

$$NPSH_i = (p_{0,\text{ref}} - p_{\text{min}})/(\rho g) \quad (6)$$

For  $p_{0,\text{ref}} = 0$  this simply becomes

$$NPSH_i = p_{\text{min}}/(\rho g). \quad (7)$$

## 3 Analysis of existing first-stage impeller design

The existing pump was designed for a rated flow of 19 500 gpm (4430 m<sup>3</sup>/h). This two-stage double-suction pump is used for injecting water into oil fields at a total pressure gain of 3265 ft (995 m). The pump runs at a rotational speed of 4800 rpm, and has been placed behind a booster pump delivering a rated head of approximately 400 ft (122 m); this being also the available *NPSH* for the pump considered. The required *NPSH* for the main pump (at 3 percent head drop) at duty flow was rated at 175 ft (54 m).

As already mentioned in the introduction, the two first-stage impellers of this pump suffered from premature wear due to cavitation attack. Within 10 000 hours of operation severe erosion has occurred at the hub and suction side of the impeller vanes just after the leading edges, as identified in Fig. 2.

Since there is enough *NPSH* available to meet the requirements as specified on the original pump performance curves, there was adequate reason to employ three-dimensional computational-fluid-dynamics (CFD) calculations to investigate the discrepancy, and figure out the root cause(s) for the cavitation occurring in the first-stage impellers of this pump.

### 3.1 Geometrical description of existing first-stage impeller

A three-dimensional model of the first-stage impeller was generated in several steps. Starting point for generating the three-dimensional model was the original two-dimensional pattern drawing, from which the full-size impeller was constructed. Next, the model for the existing impeller was derived from the full-size model, by cutting back the vanes

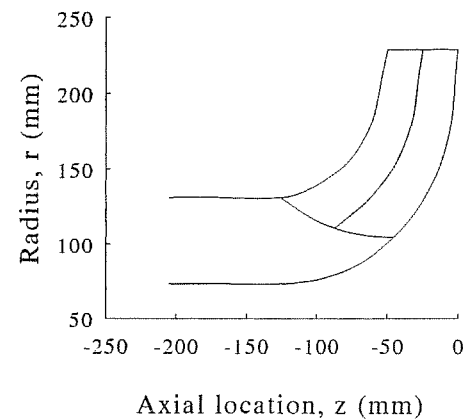


Fig. 4. Meridional ( $r, z$ ) view of existing impeller

over 5°. Furthermore, the thickness distribution at the leading edge was modified in line with the field situation.

Because of the double curvature of the vanes, the model is described by three construction lines, defining the three-dimensional geometry. Each construction line consists of a number of construction points for which the radius  $r$ , the axial coordinate  $z$ , the blade angle  $\beta$  and the blade thickness  $\delta$  are given. In this way, the three-dimensional model is determined by meridional coordinates (Fig. 4) and a blade angle distribution for each construction line (Fig. 5). The resulting three-dimensional model of the existing impeller, as used for the three-dimensional numerical flow-field analysis, is shown in Fig. 6.

### 3.2 Three-dimensional numerical flow-field analysis of existing first-stage impeller

From the three-dimensional impeller geometry, a grid was generated consisting of 21 300 nodes, with grid refinement near the vane edges. With this grid, computations have been performed for flow rates varying from 30 till 200 percent of the rated value (19 500 gpm). For this flow range the incipient *NPSH* has been determined as described (Sect. 2.2.2). The results are displayed in Fig. 7, which also shows the originally measured *NPSH* required (that is, at three percent head drop).

Figure 7 shows that the value of the best cavitation point (BCP) lies at about 160 percent of the rated flow. The reason for this high flow rate at which the BCP occurs is that the entrance blade angle of the middle construction line is far too high. It exceeds the hub and shroud angles with more than 20 percent (see also Fig. 5). This high value emerged because this middle construction line was never considered in the original design (which dates back to the early 70's). Figure 7 further indicates that there will be cavitation for the entire operating range, considering that the (rated) *NPSH* available is about 120 m.

Lastly, to indicate the influence of blade shape and flow rate, Fig. 8 displays the pressure distribution in the impeller

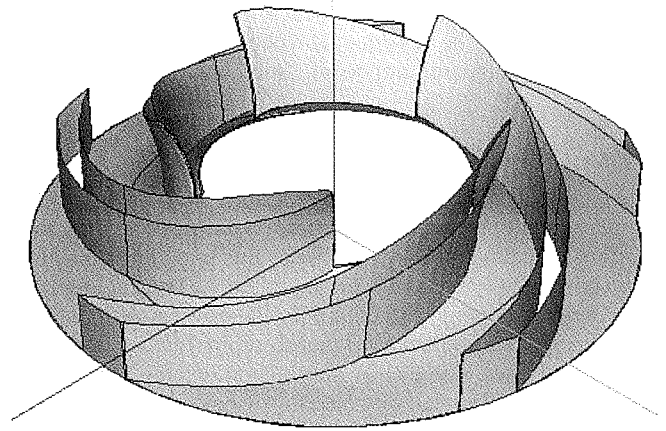


Fig. 6. Resulting three-dimensional model of existing impeller for finite element computations of impeller flow field

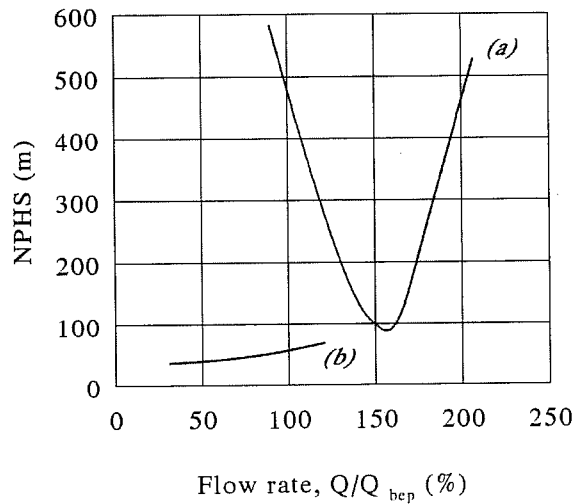


Fig. 7. *NPSH* curves of the existing design as function of the Best Efficiency Point (BEP) volume flow rate; (a) computed incipient *NPSH*, (b) measured *NPSH*<sub>3%</sub>

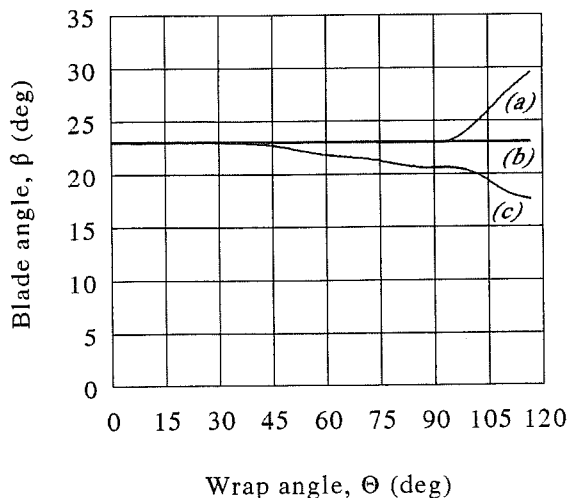


Fig. 5. Blade angle distribution of existing design with respect to wrap angle; (a) middle construction line, (b) hub construction line, (c) shroud construction line

at 80 percent of the rated flow. It shows the regions where the pressure is below vapour pressure for the situation that the *NPSH* available equals 400 ft (120 m). In these regions one typically would expect vapour filled cavities, and, hence, long cavitation bubbles will be present along the hub, causing severe damage. It should further be recognized that the shape of the regions identified in Fig. 8 corresponds with the damage patterns observed (Fig. 2).

### 3.3 Concluding remark

The foregoing analysis of the existing impeller design has identified the root cause of the cavitation damage observed. The main underlying reason being the best cavitation point (BCP) lying too far off design, i.e. at 160 percent of the rated flow, due to a far too high leading-edge blade angle at the mid construction line. The new design should have its BCP much closer to the duty point, so that cavitation will be minimized or even avoided at duty flow. A new design that will accomplish this will be discussed in the next section.

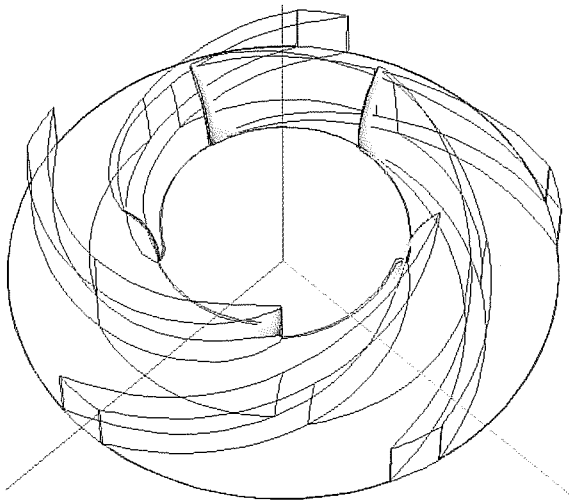


Fig. 8. Below vapour pressure regions in existing impeller at 80 percent of the rated flow and 120 m *NPSH* available

#### 4 New first-stage impeller

Here, attention will be confined to the new first-stage impeller, designed specifically to reduce (premature) wear due to cavitation attack. A brief description will be given of the new impeller geometry, and the computed cavitation performance of the new impeller will be presented.

##### 4.1 Geometric description of new design

The main differences between the new and the existing impeller design, influencing cavitation performance, are:

- (a) Decrease of the inlet blade angles (Fig. 10).
- (b) Decrease of the vane thickness (by 40 percent).
- (c) Different geometry of the leading edge (“forward-swept and elliptic-profiled nose”).
- (d) Different blade angle distribution (Fig. 10).

Figures 9–11 identify the resulting geometry of the new impeller.

##### 4.2 Performance of the new impeller design

The cavitation performance of the new impeller design has been numerically analyzed like the existing design. The first thing to look at, is how the *NPSH* required, that is the incipient value, has changed from the existing design to the new design. Figure 12 shows that the best cavitation point has shifted from 160 percent of the rated flow for the original impeller to about 100 percent of the rated flow for the new design. Furthermore, it can be seen that the minimum value of the incipient *NPSH* has decreased a little bit. Taking this into account it can be concluded that the pump will run free from cavitation around duty flow with the new first-stage impeller.

The numerical calculation further showed for 80 percent duty flow that the region where cavitation will be occurring when there is 400 ft (120 m) *NPSH* available has diminished dramatically for the new designed impeller. In fact, with the

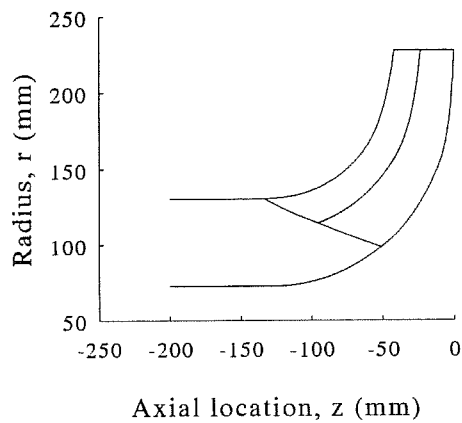


Fig. 9. Meridional (*r, z*) view of new impeller design

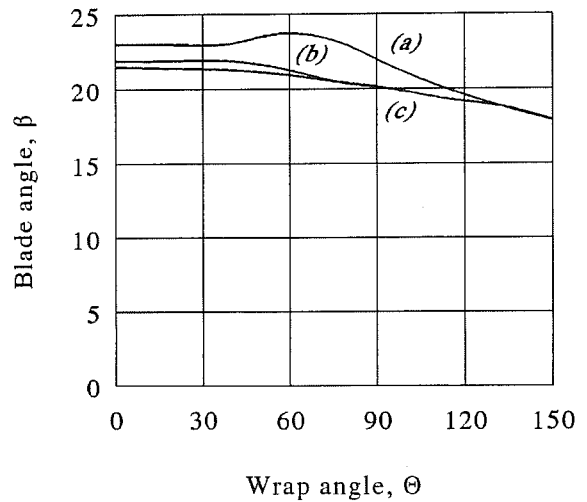


Fig. 10. Blade angle distribution of new impeller design with respect to wrap angle; (a) hub construction line, (b) middle construction line, (c) shroud construction line

new design it was found that there is no occurrence of cavitation for flow rates from approximately 85 till 110 percent of the rated flow.

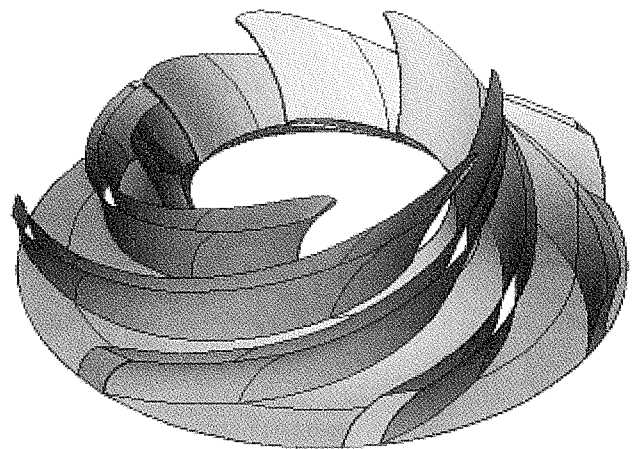


Fig. 11. Three dimensional view of new impeller design

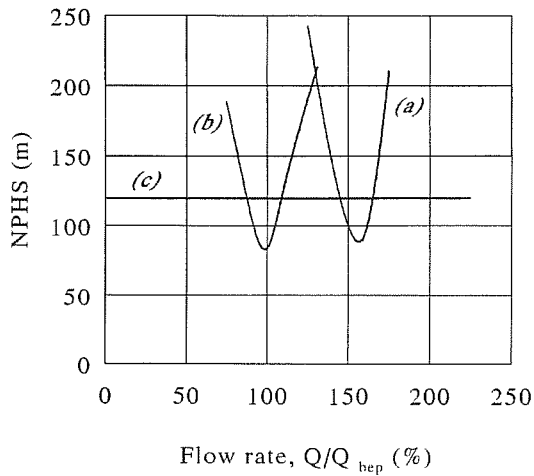


Fig. 12. NPSH curves for new design and existing design; (a) computed incipient NPSH of existing design, (b) computed incipient NPSH of new design, (c) NPSH available

## 5 Concluding remarks

A detailed numerical flow-field analysis has been discussed, identifying the root cause of severe cavitation erosion patterns observed in the first-stage impellers of a two-stage dual-first-stage centrifugal pump. These erosion patterns typically occurred within one year of operation. The root cause identified was a too high blade entrance angle, which yielded a best cavitation point at 160 percent of the rated flow.

To solve this cavitation problem and reduce the resulting premature wear, a new first-stage impeller design has been presented. This new impeller has its best cavitation point near the rated flow, and is predicted to be free from cavitation for flow rates ranging from 85 till 110 percent of the rated flow.

The findings presented have all been based on three-dimensional numerical flow-field calculations, employing the potential-flow approximation of the governing equations. This approach simplifies the flow problem (mathematically), while leaving the (physical) essentials intact.

## References

1. Batchelor, G.K.: An Introduction to Fluid Dynamics. Cambridge University Press (1967)
2. Brennen, C.E.: Hydrodynamics of Pumps. Oxford University Press (1994)
3. Kruyt, N.P., Van Esch, B.P.M., Jonker, J.B.: A tool for the analysis of unsteady potential flows in centrifugal and mixed-flow pumps. Paper C8-2. In: Proc. Pumpentagung, Karlsruhe, Germany, VDMA-Verlag (1996)
4. Lighthill, J.: An Informal Introduction To Theoretical Fluid Mechanics. Oxford University Press (1989)
5. Van Esch, B.P.M., Kruyt, N.P., Jonker, J.B.: An efficient method for computing three-dimensional potential flows in hydraulic turbomachines. In: Proc. Finite Elements in Fluids – New Trends and Applications, Venice, Italy (1995)
6. Van Os, M.J., Jonker, J.B., Op de Woerd, J.G.H.: A geometric model for the parametric design of pump impellers. Paper C5-3. In: Proc. Pumpentagung, Karlsruhe, Germany, VDMA-Verlag (1996)
7. Van Os, M.J., Op de Woerd, J.G.H., Jonker, J.B.: A parametric study of the cavitation inception behaviour of a mixed-flow pump impeller using a three-dimensional potential-flow model. Paper FEDSM97-3374. In: Proc. 1997 ASME Fluids Engineering Division Summer Meeting, Vancouver, Canada (1997)